Electronic Supplementary Material (ESI) for RSC Advances

Supplementary Information

Molecular and Continuum Hydrodynamics in Graphene Nanopores

M. E. Suk and N. R. Aluru

Department of Mechanical Science and Engineering, Beckman Institute for Advanced Science and Technology, University of Illinois at Urbana-Champaign, Urbana, IL 61801

1. Water velocity profile in the axial direction

Figure S1 shows the averaged velocity of water in the axial direction. *z* is the axial direction and the center of carbon atoms consisting of graphene nanopore is located at z=6 nm. Inset of Figure S1 is a closer view of the velocity profile inside the pore (z=5.83~6.17 nm, $\Delta z=\sigma_{cc}$=0.34 nm). Velocity variation inside the pore is negligible. Thus, $\mathrm{d}u/\mathrm{d}z \approx 0$ in the pore.

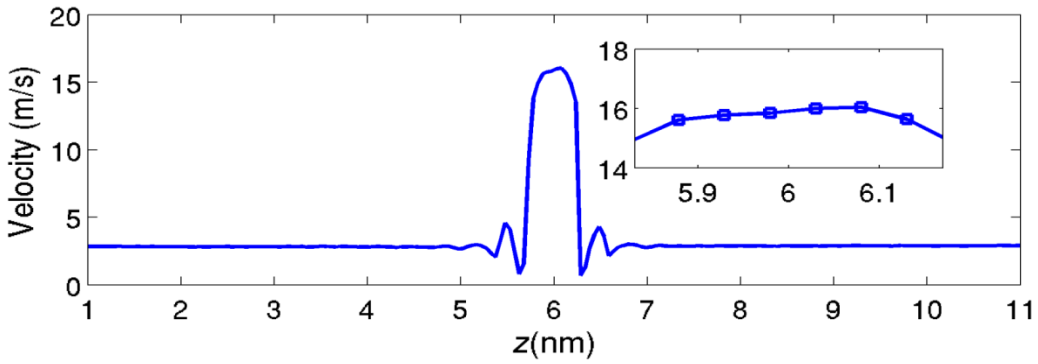

Figure S1. Averaged water velocity in the axial direction. Velocity is averaged over water molecules found inside the cylindrical bin whose radius corresponds to pore radius. In this case, pore radius, R=1.89 nm.

2. No-slip Hydrodynamics by Dagan *et al.*

Dagan et al.[1] solved creeping flow through a pore of finite length with no-slip boundary condition. The relation between volumetric flow rate and total pressure drop was approximated by

$$\Delta P_{total} = \left(\frac{3\mu}{R^3} + \frac{8\mu L_p}{\pi R^4}\right) Q$$

The first term is Sampson's solution for creeping flow through a circular orifice of zero thickness [2]. Thus, it represents pressure loss due to the entrance and exit effect. The second term is Hagen-Poiseuille's solution for flow through cylindrical pore of length L_p without entrance and exit effect. Thus, it represents pressure drop across the pore length L_p. Total pressure drop can be divided into entrance/exit pressure loss (ΔP_{loss}) and pressure drop across the pore (ΔP_p),

$\Delta P_{loss} = \frac{3\mu}{R^3} Q$ and $\Delta P_p = \frac{8\mu L_p}{\pi R^4} Q$

We defined hydrodynamic length as, $L_h = L_p \frac{\Delta P_{total}}{\Delta P_p}$. Hence, according to Dagan's approximation, $L_{h,no-slip} = \frac{3}{8}\pi R + L_p$. It shows linear relation between L_h and pore radius R.

3. Calculation of viscosity and slip length using NEMD and Green-Kubo relation

Water transport properties such as viscosity μ and slip length δ have been obtained using non-equilibrium molecular dynamics (NEMD) and equilibrium molecular dynamics (EMD) simulations. In an NEMD simulation, liquid flow is driven by an external field such as gravity, pressure gradient or shear stress and liquid properties can be calculated by comparing the velocity profile to standard models such as Poiseuille's flow[3] or Couette flow[4]. On the other hand, in an EMD simulation, liquid properties have been obtained by applying Green-Kubo (GK) relations[5, 6], which are expressed as auto-correlation functions of variables fluctuating at equilibrium. In certain cases, these methods can result in inaccurate liquid properties. For example, in the case of liquid flow showing a large slip length, such as water flow through a CNT, fluid velocity profile is almost plug-like[7, 8] and viscosity obtained by fitting the water velocity to Poiseuille's model can result in a significant error. Similarly, GK relation may not provide an accurate slip length when a large driving force is applied since slip length is reported to increase significantly beyond a critical shear rate[9]. To obtain accurate water properties, we used both NEMD and EMD simulations.

3.1 EMD method (Green-Kubo relations)

Shear viscosity can be computed from the EMD simulation via the fluctuations of the off-diagonal elements of the pressure tensor, as represented by the GK relation,

$$\mu_{\alpha\beta} = \frac{V}{k_B T}\int_0^{\infty}\left\langle \mathrm{P}_{\alpha\beta}(t_0)\mathrm{P}_{\alpha\beta}(t_0+t)\right\rangle \mathrm{d}t$$

where $\mathrm{P}_{\alpha\beta}$ are the off-diagonal elements of the pressure tensor with α, β representing the x, y or z direction and V is the volume. To avoid inaccuracies coming from long time correlations, GK relation for the viscosity can be replaced by the Einstein relation[5, 10],

$$\mu_{\alpha\beta} = \lim_{t\to\infty}\frac{V}{2k_B T}\frac{\mathrm{d}}{\mathrm{d}t}\left\langle \Delta G_{\alpha\beta}^2(t)\right\rangle$$

where $\Delta G_{\alpha\beta}(t) = \int_0^t \mathrm{P}_{\alpha\beta}(t')\mathrm{d}t'$. To calculate the local viscosity, pressure tensor should be calculated locally by utilizing

$$\mathrm{P}_{\alpha\beta} = \sum_i^M \frac{p_{i\alpha}p_{i\beta}}{m_i} + \frac{1}{2}\sum_i^M\sum_{j\neq i}^N r_{ij\alpha}F_{ij\beta}$$

where i is an index of atom inside the bin, M is the number of atoms inside the bin, j is index of all atoms in the simulation box, N is the total number of atoms in the simulation box, and p_i and m_i are momentum and mass of atom i, respectively, r_{ij} and F_{ij} are the distance and force between atom i and j, respectively, α and β are dimensional components (α,β=x,y,z).

To calculate local viscosity in graphene nanopore, graphene pore region was defined as a cylindrical bin whose length is L_h (defined in the main article) and radius equal to the pore radius. Flow was in the z-direction. Thus, suitable components of pressure tensor are xz=yz=zx=zy. We obtained $<\Delta G_{\alpha\beta}^2(t)>$ as shown in Figure S2. Between 2ps to 5ps, $<\Delta G_{\alpha\beta}^2(t)>$ was linearly fit to obtain the slope. From the slope of the linear fit, viscosity was calculated. Average and standard error of viscosity were obtained from the four components of viscosity. We calculated viscosity in the bulk region to check our calculation. We obtained a value of 0.00085 Pa·s, which is in good agreement with experimental data[11].

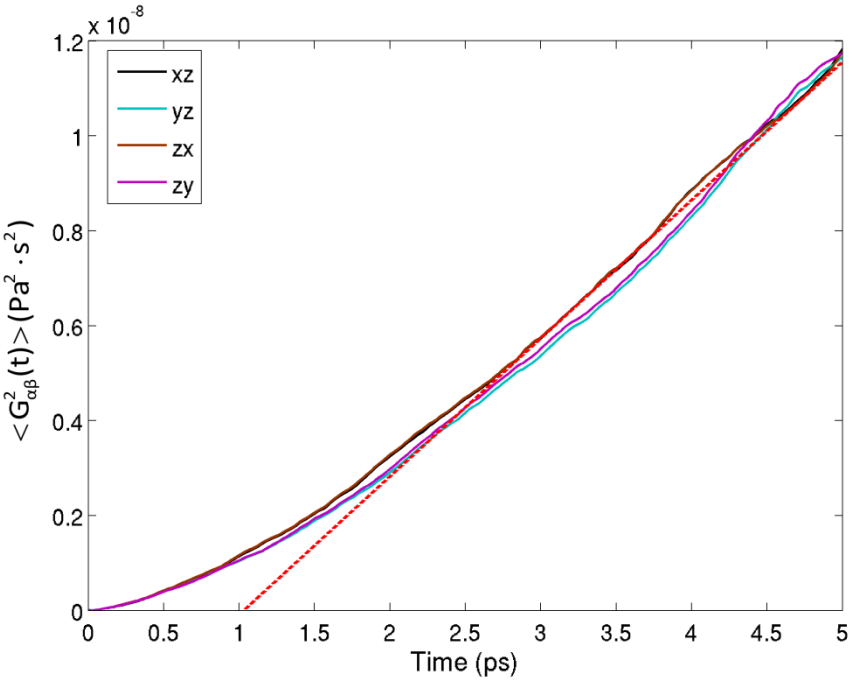

Figure S2. $<\Delta G_{\alpha\beta}^2(t)>$ calculated in graphene pore region. Each line indicates αβ=xz, yz, zx, or zy. Red dashed line is a linear fit from 2 to 5 ps. All the four components are used to obtain the mean and standard error of viscosity. In this case, graphene nanopore radius is 1.169 nm

In an EMD simulation, the friction coefficient, λ, can be obtained from the auto-correlation function (ACF) of the total force acting on the surface as[12],

$$\lambda = \frac{1}{Ak_BT}\int_0^\infty \langle F_z(t)F_z(0)\rangle dt$$

where $A=2\pi RL_p$ is the surface area, k_B is the Boltzmann constant, T is the temperature and F_z is the total force acting on pore surface in the axial direction. F_z is calculated by summing the force acting on the edge atoms defining graphene pore. Edge atoms defining graphene pore are considered as the atoms whose number of bonded neighbor atoms is less than three since carbon atoms consisting of bulk graphene have three bonded neighbor atoms. Then, δ is related to λ by δ=μ/λ. ACF of the total force and the cumulative integration of ACF are plotted in figure S3(a) and figure S3(b) respectively. ACF approaches to zero within 5ps. The friction coefficient was calculated from a constant fit on the plateau between 4 ps to 5 ps of Figure S3(b).

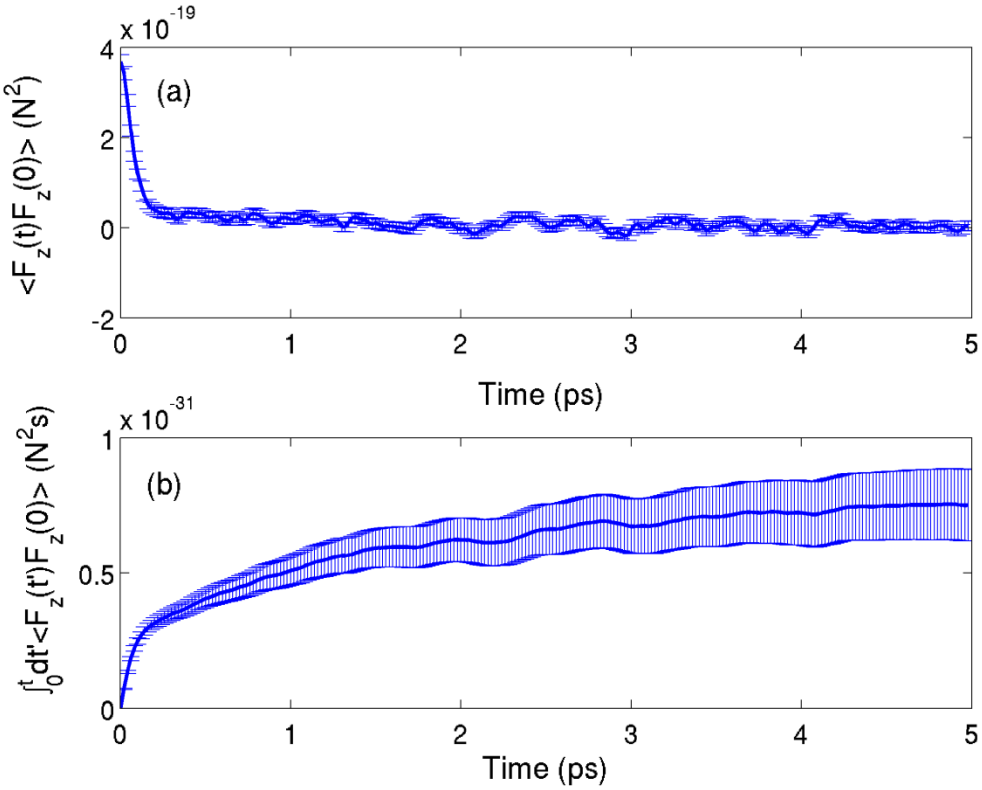

Figure S3. (a) Auto correlation function (ACF) of the total force acting on the graphene pore surface and (b) cumulative integration of ACF. Friction coefficient is obtained from the constant fit of plateau between 4 ps and 5 ps. In this case, graphene nanopore radius is 1.169 nm

3.2 NEMD method

We also calculated μ and δ from NEMD simulations by fitting velocity profiles to corrected Hagen-Poiseuille's equation,

$$u(r) = \left(-\frac{1}{4\mu} r^2 + \frac{R^2}{4\mu} + \frac{R}{2\mu}\delta \right) \frac{\Delta P_{\text{total}}}{L_h}$$

These are compared to μ and δ obtained from the EMD simulation in Figure 3(a) and 3(b) in main article. δ is an intrinsic property of the interface that describes the fluid boundary condition [13]. It also determines the amount of surface frictional shear stress, $\tau_w = \mu u_z(R)/\delta$, when slip occurs ($u_z(R) \neq 0$). In the linear Navier boundary condition[14], when the shear rate is smaller than the critical shear rate[9], δ is constant. As shown in Figure 3(b), δ obtained from the NEMD

simulation does not vary with the applied pressure drop up to 300 MPa. Also, it is in good agreement with δ=0.313 nm, obtained from the EMD simulation.

Chen *et al.* [15] reported that the viscosity of water confined in an infinite CNT decreases with increasing flow rate. However, we found no conclusive evidence that viscosity depends on the applied pressure drop or flow rate from our NEMD simulations. As shown in Figure 3(a), μ obtained from the NEMD simulation can be considered to be constant (within statistical variance), which is in good agreement with μ=0.00151 Pa·s, obtained from the EMD simulation. The linear relation between water flux and the applied pressure drop found in this study also implies that both the slip length and viscosity are constant.

Chen *et al.* calculated viscosity from $\mu_{\text{no-slip}} = \tau_w R/(4\bar{u})$, where the wall shear stress is $\tau_w = \Delta P R/(2L)$. This relation was obtained from the water flow rate, $Q = \pi R^4 \Delta P/(8\mu L)$, assuming no-slip boundary condition at the wall. If the slip boundary condition is considered, $\mu_{\text{slip}} = \tau_w \delta/(\bar{u})$, since $u(R) \approx \bar{u}$ for the CNT. Although it is possible that varying viscosity with flow rate reported by Chen *et al.*[15] is due to the effect of non-constant slip length, this needs further investigation. In prior work, constant water viscosities (bulk water viscosity[7, 16] or corrected viscosity for nanoscale[3, 17]) have been used to analyze liquid flow at nanoscale.

4. Definition of pore radius and length

Calculation of μ and δ can be sensitive to the small change in pore radius R and pore length L_p. In addition, calculation of flow enhancement[16], used to characterize the efficiency of membranes, also depends sensitively on the definition of the pore radius[17]. Thus, a proper and consistent definition of the pore radius and length is necessary. At nanoscale, pore radius and length have been defined using various ways. Thomas and McGaughey[17] defined the CNT pore diameter as the distance between atomic centers of carbon consisting of CNT (D_{cc}). Thus, radius of the carbon atom is not considered in determining the pore diameter. Falk *et al.*[6] defined the pore diameter by subtracting σ_{cc} from D_{cc} where σ_{cc} is the Lennard-Jones (LJ) parameter representing diameter of carbon. Joseph and Aluru[7] defined the pore diameter by subtracting $2\sigma_{cc}$ from D_{cc}. In this case, diameter is the distance between water density peaks near the surface. The various definitions we used are listed in Table S1 and graphically depicted with the water density plot in Figure S4.

Definition No.	L_{pore}	D_{pore}
1	σ_{oc}=0.328	$D_{cc}-\sigma_{oc}$=2.421
2	σ_{cc}=0.339	$D_{cc}-\sigma_{cc}$=2.410
3	$l_{density}$=0.535	$D_{density}$=2.338
4	$2\sigma_{oc}=0.656$	$D_{cc}-2\sigma_{oc}$=2.093
5	$2\sigma_{cc}$=0.678	$D_{cc}-2\sigma_{cc}$=2.071

Table S1. Various definitions of pore length and diameter. D_{cc} is the averaged diameter based on the center of carbon atoms (center-to-center diameter) . σ_{cc} and σ_{oc} are the Lennard Jones parameters of carbon-carbon interaction and water-carbon interaction, respectively. $l_{density}$ and $D_{density}$ are based on the location where the water density drops to below 2% of the bulk density as shown in Figure S4. Values for D_{pore} are shown for the case D_{cc}=2.75 nm.

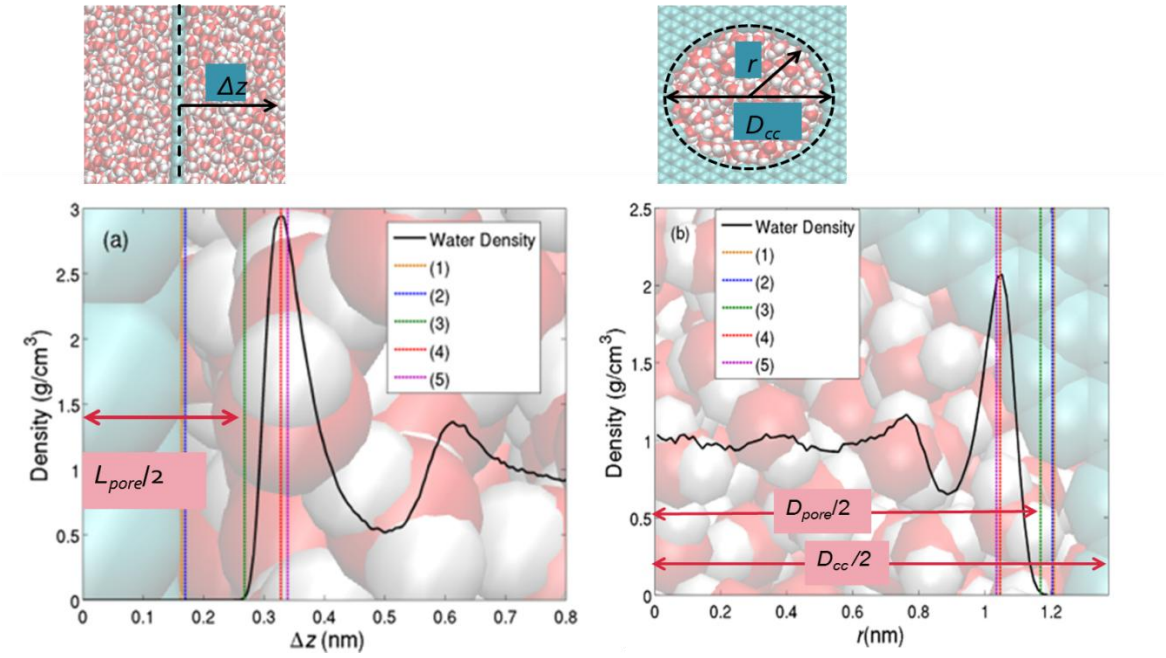

Figure S4. (a) Water density near the graphene surface. *Δz* is the distance from the center of carbon atoms consisting of graphene (see top left snapshot). Each vertical line indicates half of the graphene membrane length/thickness as defined in Table S1. (b) Water density inside the graphene nanopore in the radial direction. *r* is the radial distance from the pore center. (see top right snapshot) Each vertical line indicates the radius of the graphene pore as defined in Table S1. In this example, D_{cc}=2.75 nm.

We calculated the slip length and viscosity using each definition given in Table S1. The results are shown in Table S2. The shape and value of the velocity profile is determined by the values of the viscosity and slip length. To find the most suitable definition of the pore radius and length, we calculated the velocity profile using the corrected Hagen-Poiseuille's equation for each definition of the pore radius and length and compared the result to the molecular dynamics simulation. The comparison of the velocity profiles is shown in Figure S5. Based on these results, definition #3, where the pore radius and length are defined based on the location when the water density drops to below 2% gives the best match to molecular dynamics results. In this definition, the pore length L_p is determined to be 0.535 nm, which is slightly larger than $\sigma_{cc,}$ representing the carbon diameter.

Definition No.	Visocisty (Pa·s)	Slip length(nm)
1	0.00147	0.196
2	0.00148	0.203
3	0.00151	0.337
4	0.00148	0.381
5	0.00147	0.384

Table S2. Viscosity and slip length calculated from the Green-Kubo relation.

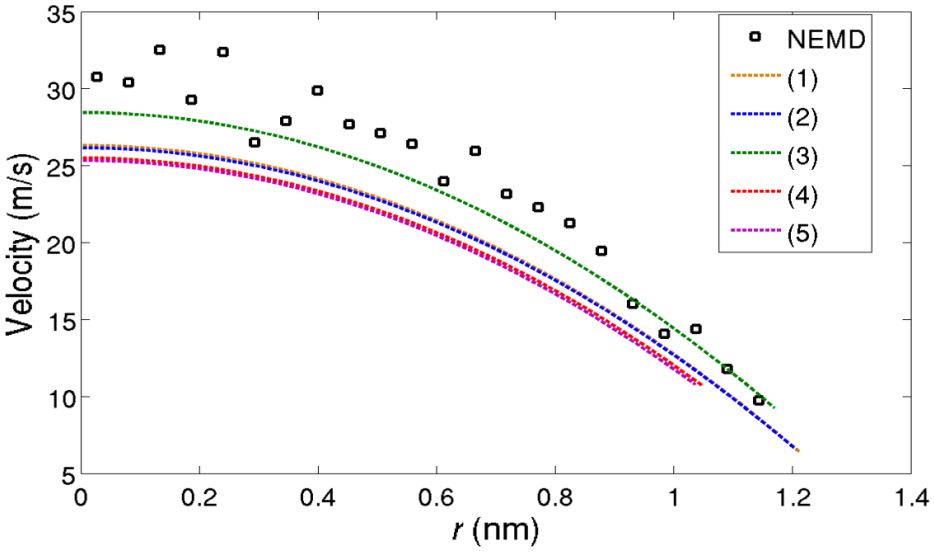

Figure S5. Axial velocity profile of water. Velocity of water is averaged inside the pore region (Δz=0.34 nm) in the case of molecular dynamics simulation. Each line is the result from corrected Hagen-Poiseuille's equation according to definition of pore radius and length. (1)~(5) represent the various definitions of pore radius and length (see Table S1 and Table S2).

5. Diffusion coefficient

According to Einsten relation, diffusion coefficient in the axial direction is given by

$$D_z = \frac{1}{2}\lim_{t\to\infty}\frac{\left\langle \left| z(t) - z(0) \right|^2 \right\rangle}{\Delta t}$$

Diffusion coefficient of water molecules in the pore region was calculated by considering water molecules in the cylindrical bin whose length is L_h (defined in the main article) and radius is the pore radius. Mean squared displacement (MSD) of water molecules inside the bin is plotted in Figure S6. A linear fit was used to obtain the slope of the MSD plot. Then, the diffusion coefficient was calculated from the slope of the MSD plot.

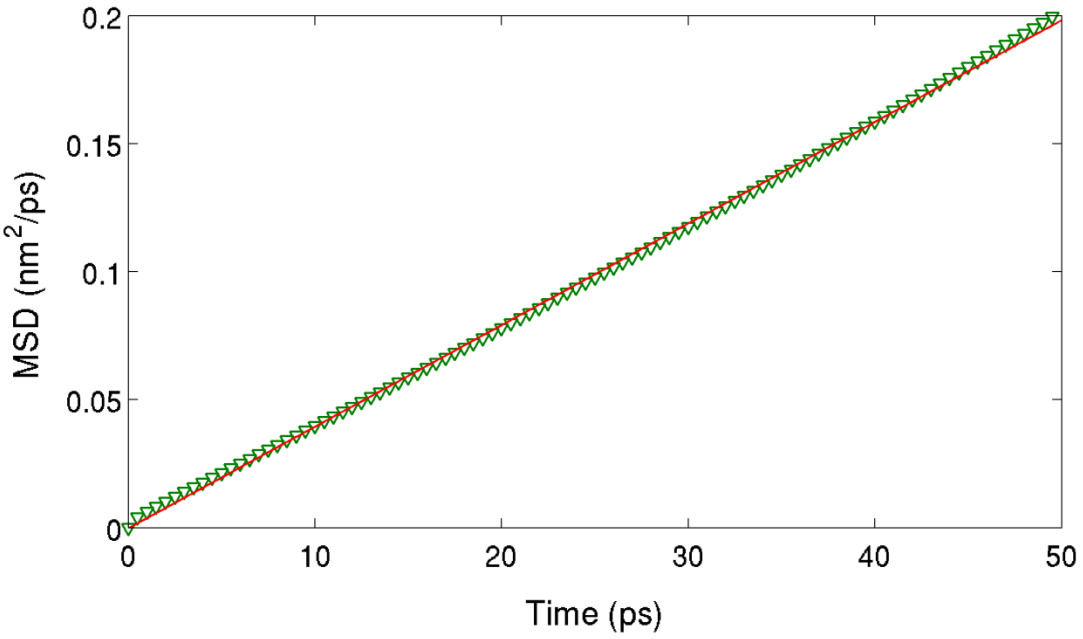

Figure S6. MSD of water molecules in the graphene pore. MSD is linear with time. The slope of the MSD was taken to calculate the diffusion coefficient.

6. Collective diffusion coefficient

The collective diffusion coeffiicent D_n is given by [18]

$$D_n = \frac{1}{2}\frac{< n^2(t) >}{t}$$

n(t) represents the cumulative flux of water molecules. *n(t)* and $<n^2(t)>$ are plotted in Figure S7(a) and (b), respectively. D_n is calculated from the slope of the linear fit in Figure S7(b).

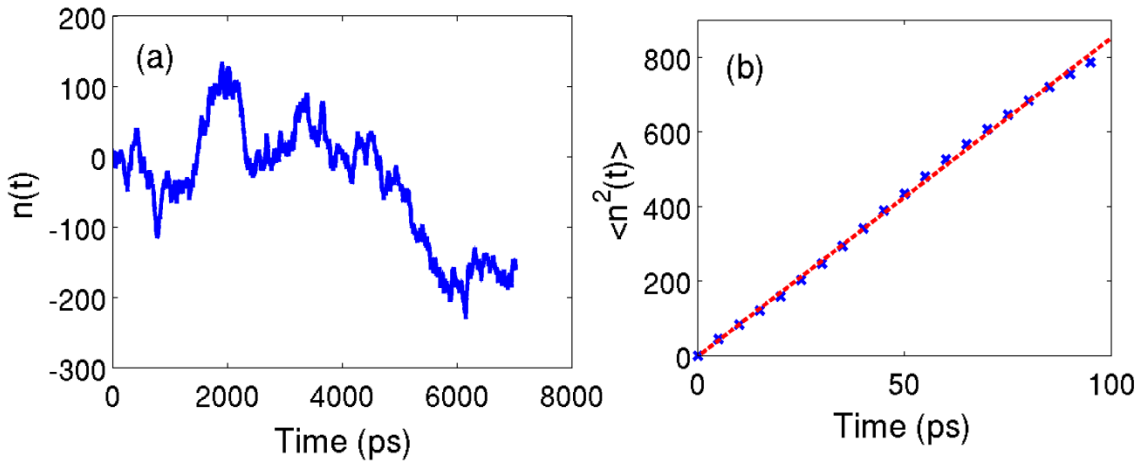

Figure S7. (a) Cumulative flux of water molecules through the graphene nanopore. When a water molecule passes through the graphene nanopore from the left to the right reservoir, n(t) is increased by +1. When a water molecule passes through the graphene nanopore from the right to the left reservoir, n(t) is decreased by 1. (b) Mean squared displacement of *n(t)*. *n(t)* is subdivided into a short time period (100 ps) and then square of *n(t)* is averaged over subdivided sections. Dashed line indicates a linear fit of data.

7. Thermal motion of graphene membrane

We investigated the effect of the thermal motion of the graphene membranes on our results. The AIREBO potential was used for the graphene membrane. Temperature of the graphene membrane and water were maintained at 300 K using Nosé-Hoover thermostat. Edge atoms of the graphene membrane were tethered to a fixed lattice site by a harmonic spring (spring constant, k=1kcal/mol) to prevent drift of the membrane[19]. Equilibrium and non-equilibrium simulation with pressure drop of 10 MPa and 300 MPa were performed. Pore structures were stable in all simulations (see figure S9 and figure S10). The velocity profile and density profile show negligible effect of thermal motion of graphene (see figure S10 and S11).

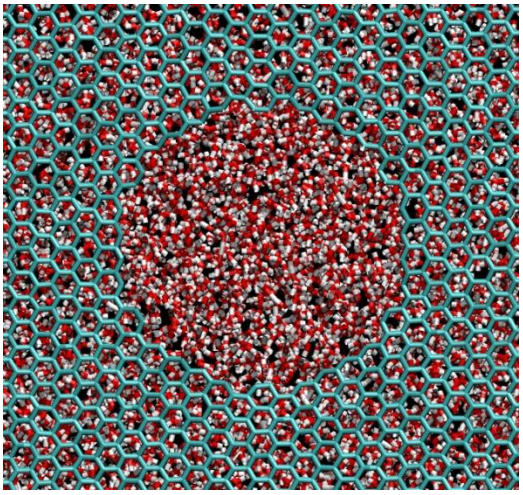

Figure S8. Random snapshot of pore structure during equilibrium simulation.

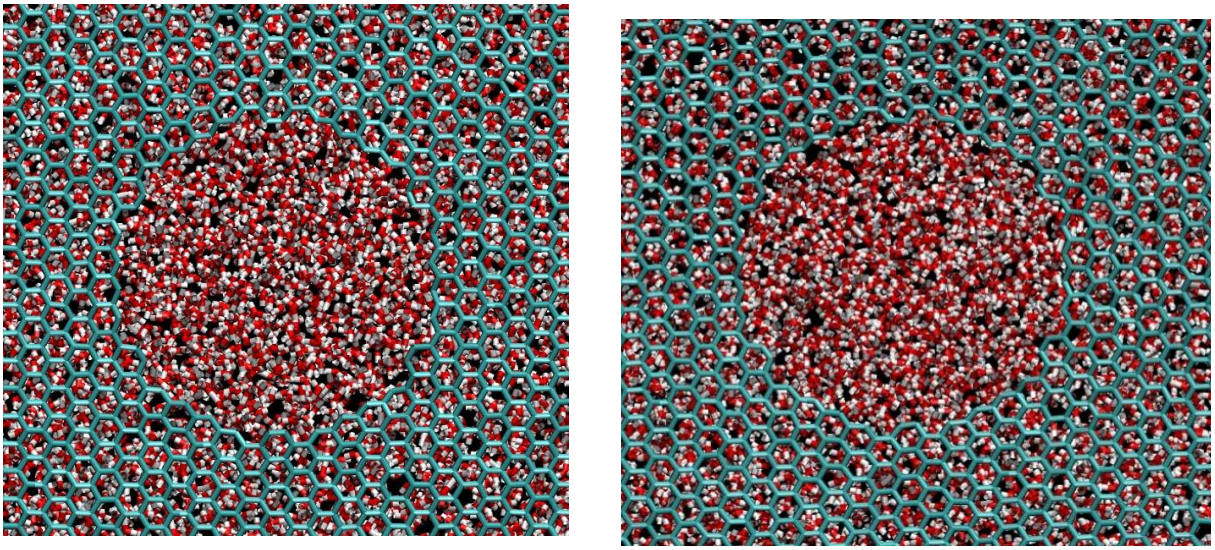

Figure S9. Random snapshot of pore structure during non-equilibrium simulation. Pressure drop of 10 MPa (left) and 300MPa (right) are applied.

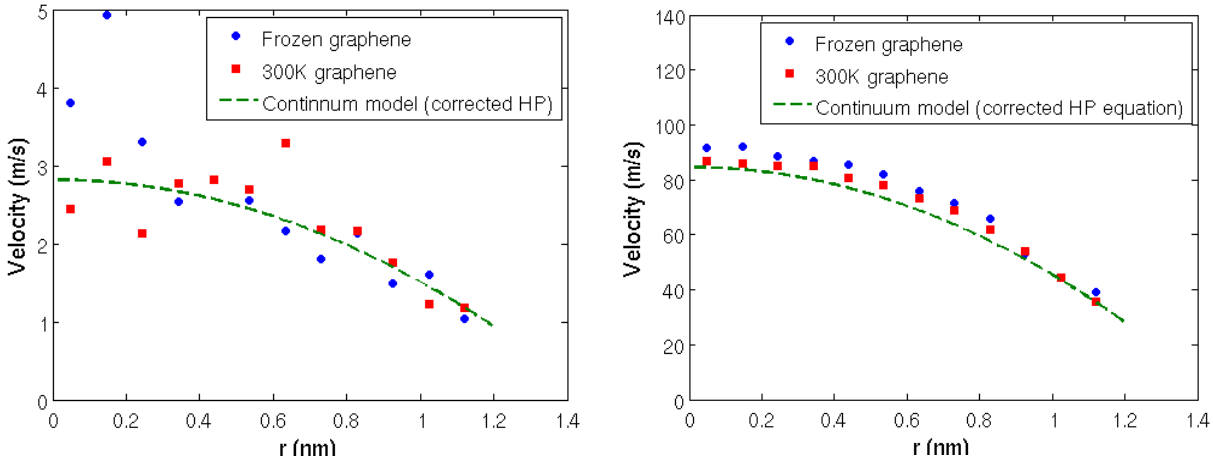

Figure S10. Velocity profile with the pressure drop of 10 MPa (left) and 300MPa (right). Under both low pressure drop and high pressure drop, there is no significant difference between fixed graphene (frozen graphene) and graphene with thermal motion (300K graphene).

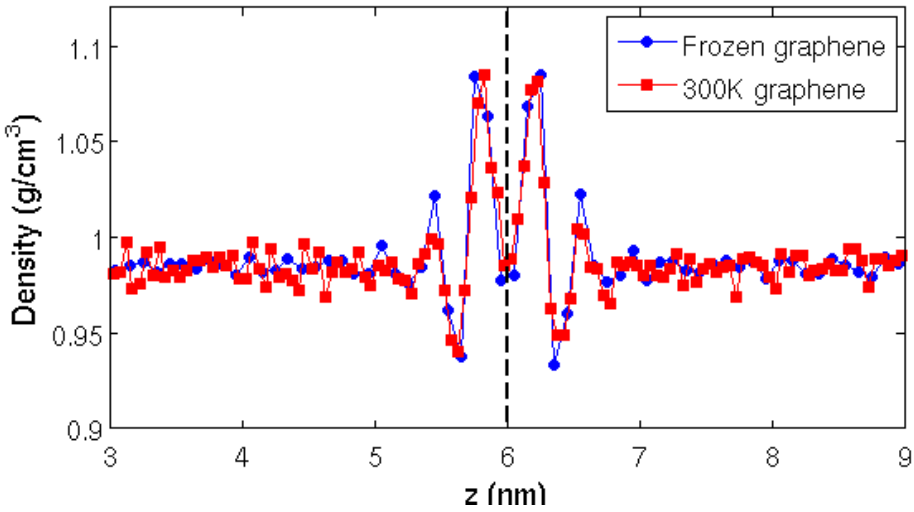

Figure S11. Density profile along axial direction in equilibrium simulation. Fixed graphene (frozen graphene) is compared to the graphene with thermal motion (300K graphene). Thermal motion of the graphene has negligible effect on the water structure

References

1. Z. Dagan, S. Weinbaum and R. Pfeffer, *J. Fluid Mech.*, 1982, **115**, 505-523.
2. R. A. Sampson, *Philos. Trans. R. Soc. Londeon, Ser. A*, 1891, **182**, 449-518.

3. V. P. Sokhan, D. Nicholson and N. Quirke, *J. Chem. Phys.*, 2001, **115**, 3878-3887.
4. T. M. Galea and P. Attard, *Langmuir*, 2004, **20**, 3477-3482.
5. B. Hess, *J. Chem. Phys.*, 2002, **116**, 209-217
6. K. Falk, F. Sedlmeier, L. Joly, R. R. Netz and L. Bocquet, *Nano Lett.*, 2010, **10**, 4067-4073.
7. S. Joseph and N. R. Aluru, *Nano Lett.*, 2008, **8**, 452-458.
8. I. Hanasaki and A. Nakatani, *J. Chem. Phys.*, 2006, **124**, 144708.
9. P. A. Thompson and S. M. Troian, *Nature*, 1997, **389**, 360-362.
10. P. E. Smith and W. F. Van Gunsteren, *Chem. Phys. Lett.*, 1993, **215**, 315-318.
11. R. C. Weast, *CRC Handbook of Chemistry and Physics*, CRC Press, Boca Raton, 1986.
12. L. Bocquet and J. Barrat, *Phys. Rev. E*, 1994, **49**, 3079-3092.
13. M. Cieplak, J. Koplik and J. R. Banavar, *Phys. Rev. Lett.*, 2001, **86**, 803-806.
14. H. Lamb, *Hydrodynamics*, Dover, New York 1934.
15. X. Chen, G. Cao, A. Han, V. K. Punyamurtula, L. Liu, P. J. Culligan, T. Kim and Y. Qiao, *Nano Lett.*, 2008, **8**, 2988-2992.
16. J. K. Holt, H. G. Park, Y. Wang, M. Stadermann, A. B. Artyukhin, C. P. Grigoropoulos, A. Noy and O. Bakajin, *Science*, 2006, **312**, 1034.
17. J. A. Thomas and A. J. H. McGaughey, *Nano Lett.*, 2008, **8**, 2788-2793.
18. F. Zhu, E. Tajkhorshid and K. Schulten, *Phys. Rev. Lett.*, 2004, **93**, 224501.
19. C. Sathe, X. Zou, J. P. Leburton and K. Schulten, *ACS nano*, 2011, **5**, 8842-8851.